Remote Sens. **2014**, *6*, 4025-4042; doi:10.3390/rs6054025

OPEN ACCESS

remote sensing

ISSN 2072-4292

www.mdpi.com/journal/remotesensing

Article

A Three-Dimensional Index for Characterizing Crop Water Stress

Jessica A. Torrion [1,*], Stephan J. Maas [2], Wenxuan Guo [3], James P. Bordovsky [4] and Andy M. Cranmer [4,†]

[1] Northwestern Ag Research Center, Montana State University, Kalispell, MT 59901, USA

[2] Department of Plant and Soil Science, Texas Tech University, 3810 4th Street, Lubbock, TX 79415, USA; E-Mail: stephen.maas@ttu.edu

[3] Monsanto Company, 700 Chesterfield Pkwy W, Chesterfield, MO 63017, USA; E-Mail: wenxuan.guo@monsanto.com

[4] Texas A&M AgriLife Research and Extension Center, 823 W US 70, Plainview, TX 79072, USA; E-Mails: jbordovs@ag.tamu.edu (J.P.B.); andy.cranmer@pioneer.com (A.M.C.)

[†] Current Address: Dupont Pioneer, 2302 SE 9th Street Hermiston, OR 97839, USA

***** Author to whom correspondence should be addressed; E-Mail: jessica.torrion@montana.edu; Tel.: +1-406-775-4303; Fax: +1-406-755-8951.

Received: 14 October 2013; in revised form: 24 March 2014 / Accepted: 15 April 2014 / Published: 2 May 2014

Abstract: The application of remotely sensed estimates of canopy minus air temperature (*Tc-Ta*) for detecting crop water stress can be limited in semi-arid regions, because of the lack of full ground cover (GC) at water-critical crop stages. Thus, soil background may restrict water stress interpretation by thermal remote sensing. For partial GC, the combination of plant canopy temperature and surrounding soil temperature in an image pixel is expressed as surface temperature (*Ts*). Soil brightness (SB) for an image scene varies with surface soil moisture. This study evaluates SB, GC and *Ts-Ta* and determines a fusion approach to assess crop water stress. The study was conducted (2007 and 2008) on a commercial scale, center pivot irrigated research site in the Texas High Plains. High-resolution aircraft-based imagery (red, near-infrared and thermal) was acquired on clear days. The GC and SB were derived using the Perpendicular Vegetation Index approach. The *Ts-Ta* was derived using an array of ground *Ts* sensors, thermal imagery and weather station air temperature. The *Ts-Ta*, GC and SB were fused using the hue, saturation, intensity method, respectively. Results showed that this method can be used to assess water

stress in reference to the differential irrigation plots and corresponding yield without the use of additional energy balance calculation for water stress in partial GC conditions.

Keywords: cotton; water stress; irrigation; remote sensing; soil brightness; ground cover; temperature; fusion technique

1. Introduction

The Crop Water Stress Index (CWSI) method for assessing water stress in plants is based on the observation that plant stomata close as a natural crop response to the depletion of soil moisture. The resulting decrease in latent heat flux from the plants gives rise to an increase in leaf and canopy temperature. Canopy temperature (*Tc*) minus air temperature (*Ta*) has been shown to be an effective indicator of crop water stress [1]. The application of *Tc*-*Ta* to irrigation management can be achieved through the use of commercially available infrared sensors that can be mounted in the field. In practice, however, measurement of *Tc*-*Ta* at a few locations may not provide an adequate indication of water stress conditions that are representative of a field, particularly if the field contains appreciable spatial heterogeneity in soil moisture conditions resulting from variation in soil physical properties. An alternative is the use of satellite- or aircraft-based remote sensing imagery within the thermal infrared (TIR) spectral range, which is capable of capturing the spatial variability in surface temperature.

Several criteria must be met for remote sensing imagery to be effective in irrigation management. These include high spatial and temporal resolutions and the delivery of the data to the user shortly after they were acquired [2]. Historically, aircraft-based imagery has been better at meeting these criteria than satellite-based imagery. Aircraft imagery can be available for analysis in a matter of hours after its acquisition. Recently, imagery from Landsat has become available on the day following its acquisition, which is an improvement in its availability from what it was in the past (1–2 weeks). However, the acquisition frequency of 16 days, plus the possible loss of images due to cloud cover, makes it difficult to directly apply Landsat data for irrigation applications. Direct application of CWSI based on remote sensing imagery has been limited to situations where the crop has attained a ground cover (GC) near 100% [3]. When the GC is significantly below 100%, the measurement of canopy temperature is confounded by the temperature of the surrounding background of plants. Thus, what is often measured by the remote sensing system is surface temperature (*Ts*), which includes the effects of plants and adjacent soil. It is common for irrigated production systems located in arid or semi-arid regions to not reach full ground canopy cover as a result of their relatively high evapotranspiration (ET) demand and lack of sufficient irrigation. For effectively using remote sensing imagery in CWSI-based irrigation scheduling, there is a need to separate the effects of the canopy and soil spectral responses [4] and account for the significant contribution of exposed soil in the surface energy balance of the crop [5].

The Vegetation Index-Temperature Trapezoid (VITT) method [6] was developed to address the problem of incomplete canopy cover. In it, a vegetation index (VI) acting as a surrogate for GC is plotted *vs. Ts*-*Ta*. In this two-dimensional space, a trapezoidal figure is identified with vertices corresponding to four critical states of the plant canopy: (1) non-stressed plants with 100% GC; (2) fully stressed plants with 100% GC; (3) wet bare soil (0% GC); and (4) dry bare soil (0% GC). The

locations of these vertices can be estimated from energy balance calculations or, in some cases, can be directly observed. It is hypothesized that all observed combinations of *Ts*-*Ta* and GC for a crop should lie within the VITT. Because the relationship between the VI and GC may be site-specific, the evaluation of the VITT at one location may not be directly applicable to other locations. This can hinder the general applicability of this method [7].

Interpretation of VI under conditions of incomplete GC is confounded by soil brightness (SB) effects. The contribution of SB to an image is determined by a number of factors, including soil parent material, organic matter and soil moisture [8–13]. When values of surface reflectance (or image digital counts) in the near-infrared (NIR) spectral band are plotted *vs.* corresponding values in the red spectral band, points representing bare soil tend to lie along a straight line in this two-dimensional space [14]. These authors showed that soils with various parent materials, textures, soil moisture contents and organic matter contents could be accommodated by a single line, commonly called the "bare soil line". The position of a soil along the bare soil line is a measure of its relative brightness and is related to factors, such as soil texture and soil moisture content. Thus, SB can provide additional information regarding the nature of the soil background.

This article presents a new approach based on the hypothesis that the inclusion of SB information as an additional dimension to the known relationship between GC and *Ts*-*Ta* will demonstrate an ability to detect and assess crop water stress. Our objectives include: (1) evaluating SB, GC and *Ts*-*Ta* from remote sensing image data for a range of crop water stress conditions; and (2) developing a fusion approach to assessing crop water stress that makes use of this information. The approach was evaluated and tested using field data for cotton (*Gossypium hirsutum* L.) from the semi-arid Texas High Plains and high-resolution airborne multispectral remote sensing imagery. In the field studies, various levels of crop water stress were established through differential irrigation over two consecutive years.

2. Materials and Methods

The study was conducted during 2007 and 2008 in the Texas High Plains at the Texas A&M AgriLife Research and Extension Center at Halfway, TX (34.184 °N, −101.940 °W). The soil at the study site is a Pullman clay loam (fine, mixed, superactive, thermic Torrertic Paleustolls) [15]. Cotton was planted on 17 May 2007, and 19 May 2008, with a rate of 100,000 seeds ha^{-1} in a 19-ha field with 1-m row spacing. The field was equipped with a low-energy precision-application (LEPA) center-pivot irrigation system. The field was circular and was divided into four 70 °sections (blocks). Each of these sections was split into three smaller wedge-shaped subplots. The 3 treatments were arranged according to a complete randomized block design within each of the four blocks. The three irrigation treatments were: (1) irrigation at 3.4 $mm \cdot d^{-1}$ (HighIrr); (2) irrigation at 1.7 $mm \cdot d^{-1}$ (LowIrr); and (3) a "dryland check", which received no irrigation (dryland). Irrigation started at the squaring stage and was applied once per week. The LEPA system had flow valves that were manually opened and closed as the pivot passed over a treatment plot to produce the desired rate. Daily values of reference ET (ET_0), crop ET (ETc), precipitation and air temperature were obtained from a weather station maintained by the Texas High Plains Evapotranspiration (TXHPET) Network [16] at the halfway location. Cumulative ETc,

rainfall and irrigation for the three treatments are presented in Figure 1 for the two study years, along with the timing and amounts of rainfall.

The *Ts* was measured hourly using four TIR (Exergen Corp model IRT/c.03, 15 ° field of view) sensors with custom-built enclosures [17] and installed on a frame placed in the plots, such that the array of sensors spanned the cotton canopy from the center of one row to the center of the next row, as shown in Figure 2. The sensors were located 20-cm apart and approximately 1-m above the ground on the frame. The average of the four TIR sensors represented an observation of *Ts*. Individual TIR sensors were calibrated by regressing their observations against corresponding temperature measurements obtained using a commercial hand-held infrared thermometer (Everest Interscience, Inc.) when both types of devices were pointed at a calibration panel with a surface reflectance of either 0.50 or 0.95 (Labsphere, Inc., Atlanta, GA, USA) positioned just below the sensor frame.

Figure 1. (**Top**) Cumulative crop evapotranspiration (ET), rainfall and applied total water (irrigation plus rainfall) for the high irrigated (HighIrr), low irrigated (LowIrr) and non-irrigated (dryland) treatments plotted *vs.* the day of year (DOY); (**Bottom**) the amount and timing of daily precipitation events. The results are presented for the 2007 and 2008 growing seasons from planting (vertical line with date) to crop maturity. Arrows indicate the dates on which airborne remote sensing imagery was acquired.

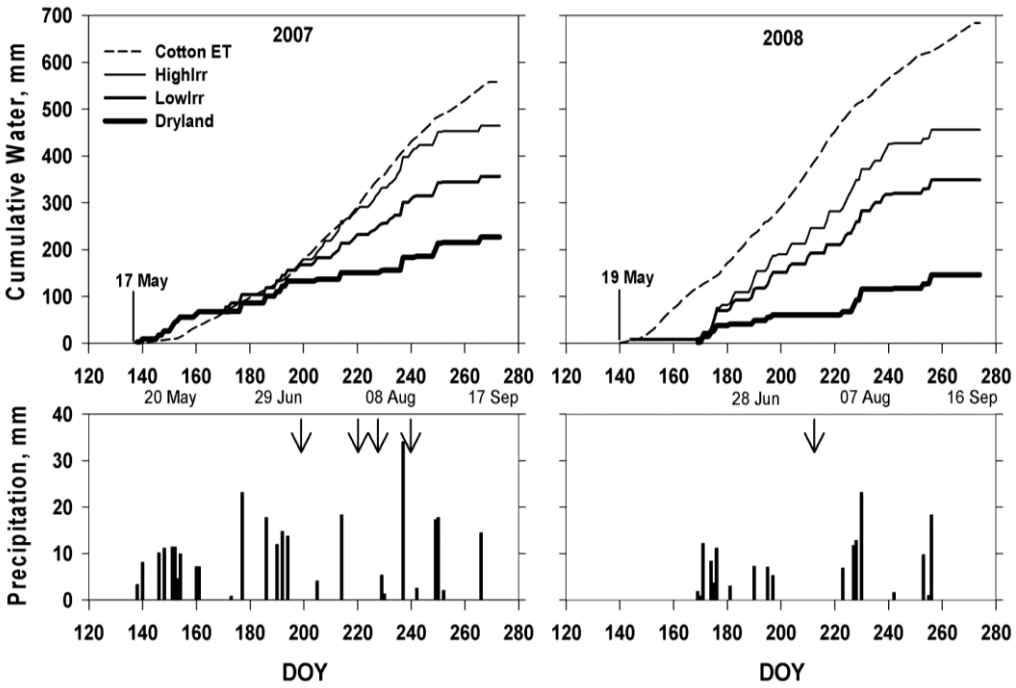

High-resolution multispectral imagery of the study plots in the red, NIR and TIR were collected on selected dates during the study. Imagery was acquired on clear days at midday using the Texas Tech Airborne Multispectral Remote Sensing System (TTAMRRS) [18]. This system was flown aboard a fixed-wing Cessna 172 Skyhawk aircraft. The aircraft was modified to allow TTAMRRS to acquire imagery in a nadir-pointing direction through a hole in the floor of the passenger cabin. Imagery was acquired at an approximate altitude of 915-m above ground to achieve a surface spatial resolution of 0.4 m for the red and NIR bands and 2 m for the TIR band.

Figure 2. Array of sensors used to monitor surface temperature (*Ts*): (**left**) high irrigation treatment; (**right**) dryland treatment.

For converting image digital counts (DC) to reflectance, a pair of calibration tarps (8 m × 8 m) with a known reflectance (9% and 60%) was used. These tarps were placed on the ground near the research field prior to the overflights of the aircraft carrying TTAMRSS so that the tarps would appear in the acquired imagery.

On the day after each remote sensing image acquisition, canopy width was measured using a meter stick at 20 random locations within each of the irrigation treatment plots. Crop GC was calculated using the following relationship,

$$GC = \frac{Cw}{Rs} \times 100 \quad (1)$$

where *GC* is expressed as a percentage, *Cw* is the measured canopy width and *Rs* is the spacing between plant rows in the field. These values were compared to corresponding estimates of *GC* obtained from the remote sensing imagery.

2.1. Image Processing

Image processing was done using ENVI software (Research Systems Inc., Boulder, CO, USA) [19]. For converting image DC values to reflectance, a linear regression equation was developed,

$$Rs = \beta(DCs) + \alpha \quad (2)$$

where *Rs* is the scene reflectance, β is the regression slope, *DC* is the digital count value for the tarp and α is the regression intercept. Equation (2) was solved separately for the red and NIR bands.

For the first image scene collected, the latitude and longitude of known ground control points (GCPs) were determined in the scene. All other acquired images were rectified by the image-to-image method based on the GCPs. The goodness of fit for the rectifications was evaluated by selecting at least 3 identifiable features (e.g., the center pivot point, road intersections and plot corners) with their corresponding X, Y coordinates in the red, NIR and TIR images [20]. The images were resampled to a common 1-m pixel size by cubic convolution. The red and NIR TTAMRSS imagery originally had sub-meter resolution, while the corresponding TIR imagery had a resolution greater than 1 m.

2.2. Calculating Soil Brightness

To determine the soil brightness associated with an image pixel representing partial canopy cover (for example, point (*X*1, *Y*1) in Figure 3), a 2D scatter plot was created by plotting red reflectance values against the corresponding NIR reflectance values. A perpendicular line (blue line in Figure 3) was drawn from point (*X*1, *Y*1) to the bare soil line (red line). In this case, the equation of the bare soil line would be:

$$Y = a0 + a1(X) \tag{3}$$

where *a*1 is the slope and *a*0 is the intercept of the soil line. The bare soil line would intercept the y-axis at the point (0, *a*0). The values for *X*s and *Y*s can be calculated from the equations [21]:

$$Xs = \frac{a1Y1 + X1 - a0a1}{a1^2 + 1} \tag{4}$$

$$Ys = \frac{a1^2 + Y1 + a1X1 + a0}{a1 + 1} \tag{5}$$

SB was determined as the distance along the bare soil line from (*X*s, *Y*s) to (0, *a*0). This distance was calculated from the equation:

$$SB = \sqrt{(Ys - a0)^2 + Xs^2} \tag{6}$$

Figure 3. Typical scatter plot of image pixel reflectances in the red and near-infrared bands.

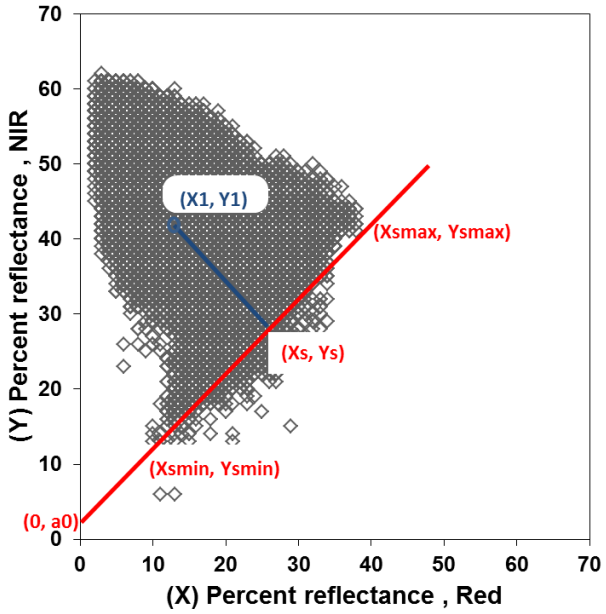

As shown in Figure 3, the point on the bare soil line corresponding to the wettest soil is (*X*smin, *Y*smin), while the point corresponding to the driest soil is (*X*smax, *Y*smax). The value of SB corresponding to the wettest soil can be calculated as:

$$SBmin = \sqrt{(Ysmin - a0)^2 + Xsmin^2} \quad (7)$$

whereas the value corresponding to the driest soil can be calculated as:

$$SBmax = \sqrt{(Ysmax - a0)^2 + Xsmax^2} \quad (8)$$

Determining the *SBmin* and the *SBmax* reference points in the imagery was achieved by referring to the multi-date reflectance values of the relatively moister and drier bare soil surfaces (e.g., center pivot pump leak, access roads and pathways between irrigation plots) that were recorded for each of the image acquisition dates. The calculated values of *SB*min (Equation (7)) and *SB*max (Equation (8)) were used to normalize the SB using the relationship,

$$SBi = \frac{SB - SBmin}{SBmax - SBmin} \times 100 \quad (9)$$

where *SBi* is the normalized SB expressed as a percentage.

2.3. Calculating Ground Cover

In order to calculate GC, the standard perpendicular vegetation index (PVI) [22] was calculated using an equation

$$PVI = \frac{[NIR - a1(Red) - a0]}{(1 + a0^2)^{1/2}} \quad (10)$$

where *a*1 and *a*0 are the slope and intercept of the bare soil line, respectively (refer to Equation (3)). Calculation of GC was based on the PVI associated with the reflectance of full canopy [7,23] as:

$$GC = \frac{PVI}{PVI_{FC}} \times 100 \quad (71)$$

where PVI_{FC} is the known PVI value for a canopy with 100% GC.

2.4. Conversion of TIR DCs to Temperature and Calculating Ts-Ta

The DCs of the TIR imagery were converted to surface temperature (*Ts*) using a linear regression between the TIR image DC of pixels and their corresponding measured temperature ground-truth TIR values at the same time the image was acquired in Figure 2,

$$Ts = \beta(TIR) + \alpha \quad (18)$$

where β and α are the regression slope and intercept, respectively. The image scene differential temperature, *Ts-Ta*, was calculated as the difference between the *T*s and air temperature (*T*a).

2.5. Fusion and Evaluation of the Relationship among SB, GC and Ts-Ta

Visualization by fusion of SB, GC and *Ts-Ta* for the research plots was carried out using ILWIS 3.31 software (ITC) [24]. In this procedure, *Ts-Ta*, GC and SB were displayed as the hue, saturation and intensity (HSI) color model, respectively. The HSI color model is a representation of human color perception; hue, dominant wavelength; saturation, purity of color; intensity, average

brightness. Respective histogram ranges assigned in the HSI color composite were 0 to 100 for GC, 0 to 100 for SB and −30 to 30 for *Ts-Ta*. These numbers represent the full range of values for GC and SB in percent, whereas the range of the *Ts-Ta* was assigned actual temperature values that resulted in consistent identification of water stress features by HSI.

To evaluate these three dimensions, the image scene was converted into a text file. Each set of GC, SB and *Ts-Ta* data in the text files were pooled into a single text file with three columns using a utility in Graphis plotting software [23]. The data values in the three columns were considered orthogonal coordinates X, Y, Z and plotted in three dimensions.

3. Results and Discussion

The seasonal average air temperature between years was similar, but some months showed variations between the years (Table 1). In 2008, May and July were warmer by 7.6 ℃ and 0.5 ℃, respectively, compared with the same months in 2007, whereas, June, August and September were slightly warmer in 2007 than in 2008. The seasonal precipitation and ET_0 varied between years (Table 1). Year 2008 received 67 mm less precipitation than 2007 and had lower monthly precipitation compared with 2007, except in June and August. Cumulative ET_0 in 2008 was 162 mm greater than in 2007, where most of the variation was due to May, which had 120 mm more than the same month in 2007. In addition, ET_0 was consistently higher from May to July in 2008 than during the same period in 2007. This higher ET demand in 2008 is also shown in Figure 1, wherein the cumulative amount of irrigation in the HighIrr treatment fell, on average, at least 100 mm below the cumulative crop ET. This resulted from the lack of rainfall received from planting to mid-June, plus the inability of the LEPA irrigation system capacity to meet the ET demand for that year. It is important to note that in 2007, the applied crop water in HighIrr treatment is close to a 100% crop ET replacement due to the higher amount of precipitation received that year.

Table 1. Seasonal and monthly air temperature, precipitation and ET_0 from the Texas High Plains ET network weather station near the study site [16].

Year	May	June	July	August	September	Season
Air Temperature (℃), Mean						
2007	18.0	22.6	23.9	24.6	21.8	22.2
2008	25.6	19.5	24.4	23.6	18.7	22.4
Precipitation (mm), Total						
2007	90	64	62	52	52	329
2008	51	80	25	70	36	262
$ET_{0\ grass}$ (mm), Total						
2007	155	190	182	176	135	838
2008	275	226	203	176	120	1000

3.1. Soil Brightness

The distribution of red and NIR pixel reflectance values in the scatter plot displayed the characteristic shape (Figure 4A), with the bare soil line lying along the diagonal lower edge and the

region of 100% GC at the upper apex. In this study, the soil line equation was not derived from the single acquisition date, but rather from several dates, so that a range of bare soil pixel values corresponding to varied soil moisture conditions could be used. The resulting soil line (*i.e.*, the regression line fit to the bare soil pixels) is shown in Figure 4B. For this soil line, relatively moist soil pixels lie along the lower left portion, while relatively dry soil pixels lie along the upper right portion. The regression slope (1.03) and intercept (7.10) are similar to the values reported in other studies [14]. This suggests that a common soil line equation might be appropriate for use in applications of this nature.

The identification of a minimum and maximum SB for use in SB normalization is not straightforward, as the brightness range can vary from image to image, as a result of the timing and magnitude of rainfall or irrigation events. The use of multi-date image data in this study allowed the identification of an SB range for use in normalizing SB that encompassed a wide range of soil moisture conditions. From the data in Figure 4B, the minimum and maximum SB were determined to be 7.0 (using Equation (7)) and 56.0 (using Equation (8)), respectively. The SB range is likely specific to a soil type, as shown by soil line data previously published for a variety of soils [14].

Figure 4. Red *vs.* NIR scatter plot of pixel reflectance from an image scene taken on 8 August 2007 (**A**), and the soil line evaluated from multi-temporal image data for georeferenced bare soil surfaces (near the pivot pump and adjacent to the plots) with varying degrees of moisture (**B**).

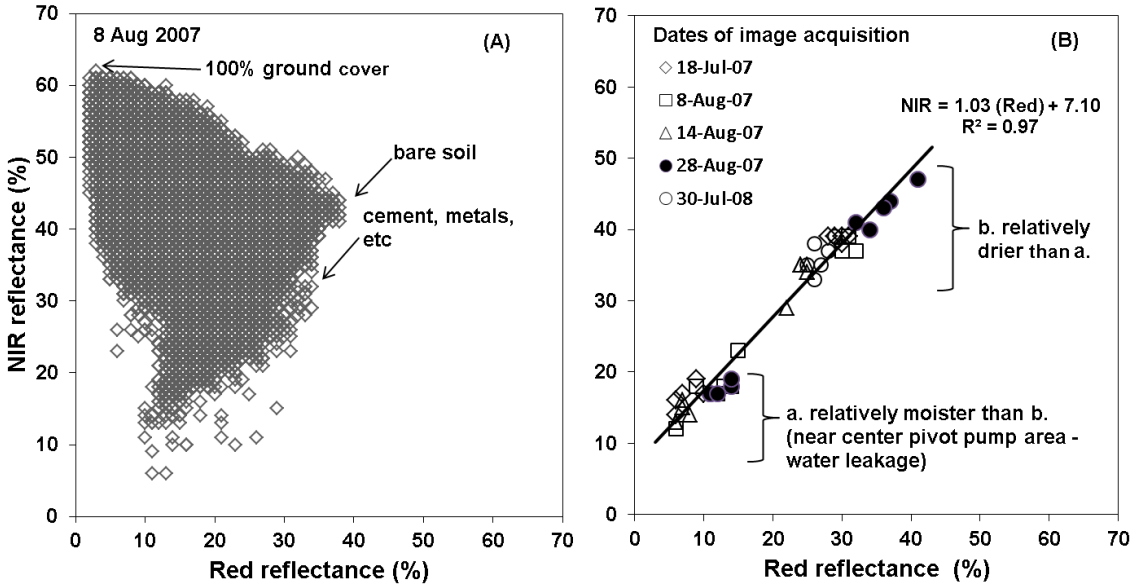

Scene SB for 2007 and 2008 is presented in Figure 5. On 8 August 2007, the wetter soil surfaces (due to excessive water released near the center of the pivot) had an SB below 20%, whereas most of the SB values shown in the rest of the image had an SB ranging from 40% to 60%. This was because, at the time of image acquisition, the pivot had just started to irrigate the northwest quarter of the field. For 21 August 2007, the calculated SB was greater (indicating drier soils) than 8 August 2007. Dryland plots in 2008 had consistently higher SB than the HighIrr and the LowIrr treatment plots. On this date, the area near the center of the pivot also had SB < 20% (similar to 8 August 2007), which demonstrates the ability of the SB method to detect moist or dry soil surfaces in this study.

Figure 5. Percent of ground cover (GC) of cotton (C) and sorghum, *Sorghum bicolor* (S), percent soil brightness (SB) and canopy minus air temperature (*Tc-Ta*) (℃), for two dates in 2007 (**A**,**B**) and 2008 (**C**) along with the respective irrigation plots for the highly irrigated (HighIrr), low irrigated (LowIrr) and dryland treatment.

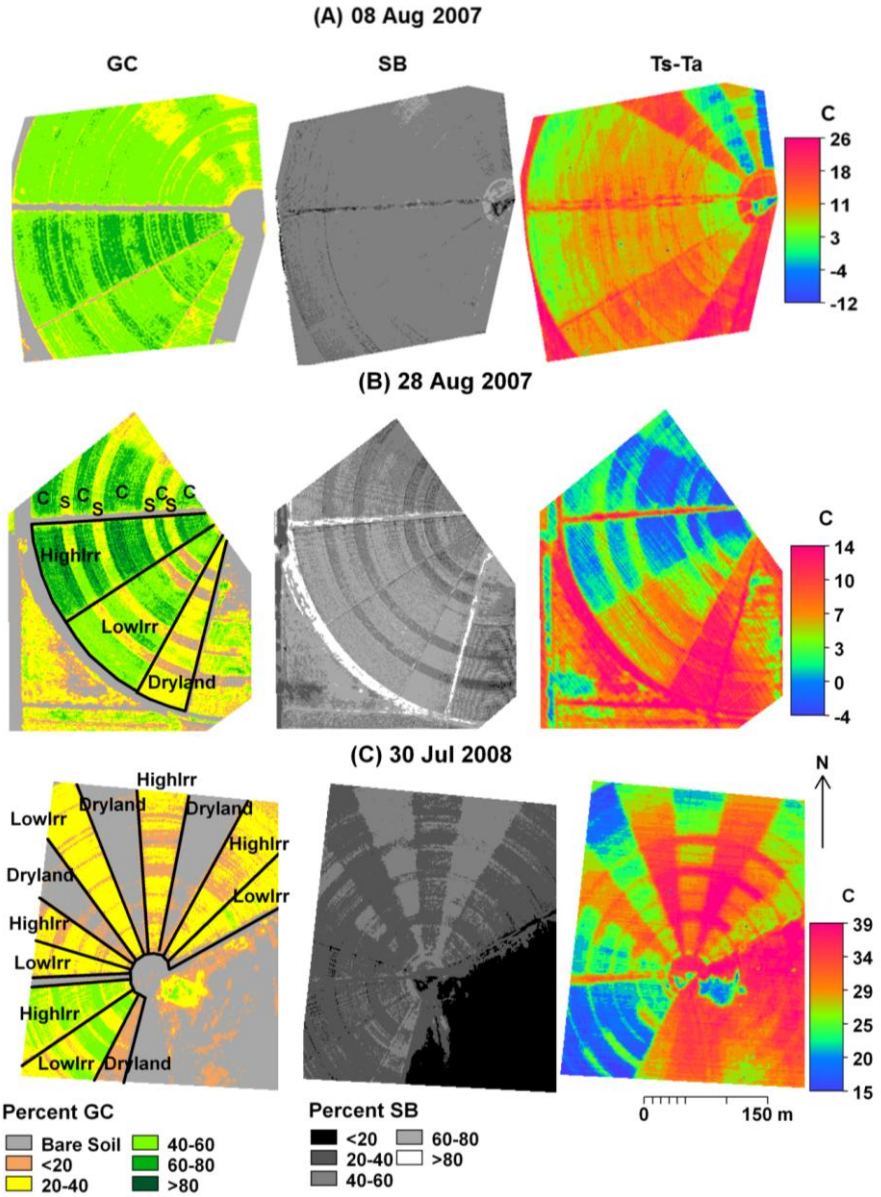

Note: sorghum was part of a 6-year (2003–2008) crop rotation and irrigation project and is out of the scope of this 2-year (2007–2008) study.

3.2. Ground Cover

An increase in GC from 8 August to 28 August in 2007 was observed in the HighIrr plot for cotton, but not for sorghum as a result of the senescence of the sorghum leaf canopy (see Figure 5). In the dryland plot, cotton GC decreased from 8 August to 28 August 2007, indicating accelerated leaf canopy senescence as compared to the HighIrr and LowIrr plots. This is an indicator that drought, in most cases, enhances crop senescence [25]. Less rainfall in 2008 resulted in incomplete GC in the

HighIrr treatment (Figure 5C), with the maximum GC ranging from 40% to 60%. Cotton plants in dryland plots were severely damaged by water stress in the northern parts of the field.

The relationship between estimated and measured GC is shown in Figure 6. Estimated and observed GC showed a good agreement (*i.e.*, 1.02 slope) and a high coefficient of determination. The slope and intercept are not statistically different from one and zero ($\alpha = 0.05$), respectively.

Figure 6. Estimated *vs.* measured ground cove (GC) for the various irrigation plots in the research site (2007–2008).

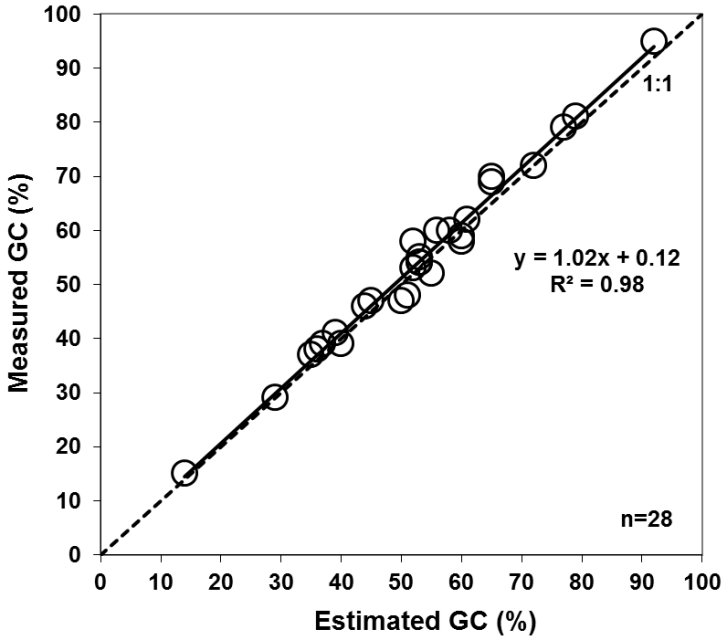

3.3. Surface and Air Temperature

The difference in *Ts-Ta* among irrigation treatment plots in both years corresponded to the amount of irrigation applied to the plots. As expected, the HighIrr treatment had the coolest average surface temperature, followed by the LowIrr treatment and the dryland plots. In 2007, plots in the portion of the field that had been irrigated by the pivot on the day the image was acquired had a surface temperature lower than or equal to the air temperature (Figure 5A,B).

High canopy temperatures in 2008 were indicative of the extreme drought conditions in that year. There was more exposed soil in 2008 than in 2007. The irrigated plots had a maximum of only 56% GC, with the exposed soil surface contributing to the increased canopy temperature through sensible heat transfer to the canopy and surrounding environment [5]. Development of the VITT approach for determining crop water stress was intended to account for partial crop canopy cover [6] in semi-arid regions, like the Texas High Plains. The *Ts-Ta* approach applied to a partial canopy situation is known to have problems, due to the effect of partial GC on the energy balance of the crop [26,27].

3.4. Fusion of Soil Brightness, Ground Cover and Temperature

Color composites of *Ts-Ta*, GC and SB assigned as hue (H), saturation (S) and intensity (I) are shown in Figure 7. The non-living features, such as bare soil, are represented in shades of gray; drier

soils appear brighter gray, whereas wetter soils appear darker gray. This representation of non-living features is an attribute of the HSI approach, whereby the fused product is considered easier to interpret by human visual perception [20,28].

With regard to crop water stress, the non-stressed crop was displayed in green, moderately stressed crop in blue and stressed crop in pink. In 2007, the dryland (non-irrigated) treatment was consistently classified as stressed (Figure 7A,B). Most of the deficit irrigation treatment (*i.e.*, LowIrr) was classified as moderately stressed, with some smaller portions classified as non-stressed or stressed. The HighIrr treatment in 2007 was generally classified as non-stressed. The HighIrr treatment in 2007 had available water (rainfall + irrigation applied) that was not markedly different from the crop ETc (Figure 1 and Table 1). Specifically, towards the end of August (28 August 2007), the HighIrr treatments were classified as non-stressed and, in some portions, moderately stressed (Figure 7B). On 8 August 2007 (Figure 7A), the same plots were classified as non-stressed or moderately stressed, with a few areas classified as stressed.

On 30 July 2008, the irrigated treatments (HighIrr and LowIrr) on the north portion of the center pivot were generally classified as stressed, with some small areas of the plots classified as moderately stressed (Figure 7C). In the southwestern portion of the field that year, both the HighIrr and LowIrr treatments were classified as stressed or moderately stressed. The cotton crop in the dryland plots in 2008 were stressed due to a lack of rainfall, and only a small number of cotton plants survived, resulting in low GC, which was mostly classified as non-living (bare soil in the north portion of the field in Figure 5C). These plots had the highest *Ts-Ta* over the three dates. The irrigated treatments (southwestern portion) were classified as either stressed or moderately stressed. At the time the image was acquired, all plants were experiencing water stress.

Figure 7. Color composites produced by hue, saturation and intensity (HIS) fusion of *Ts-Ta* (−30 ℃ to 30 ℃), GC (0–100%) and SB (0–100%) for 2007 (**A**,**B**) and 2008 (**C**).

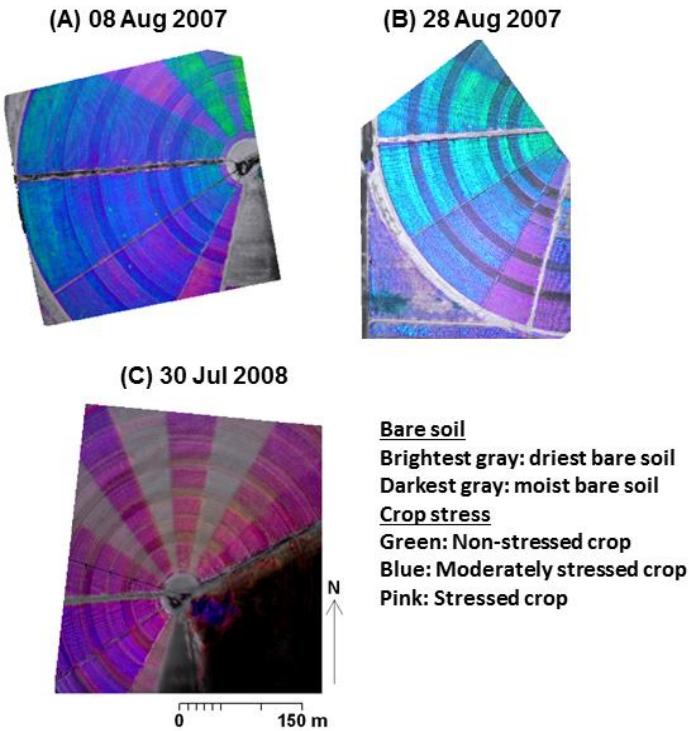

The ranges of *Ts-Ta*, GC and SB values among the three crop water stress classes are summarized in Table 2. Ranges were identified based on prior knowledge of the irrigation treatments. The HSI fused product, to some extent, corresponded to the irrigation treatments in 2007. It reliably depicted the drought conditions in 2008. For 8 August 2007, *Ts-Ta* values for the non-stressed treatment were less than or equal to zero, which would be expected for well-watered plants. Results on 28 August 2007, were not the same as those on the preceding observation in early August. In this case, the non-stressed plants showed a *Ts-Ta* value greater than zero, and if this variable were to be used for water stress evaluation, then it would have been classified as stressed to varying degrees. It can be noted that the non-stressed plants for this date had a GC range of 63%–91% with an SB range of 65%–80%. We would suggest that this is an example of the contribution of soil background effects to increased *Ts* (*i.e.*, combined plant and soil temperature).

Table 2. *Ts-Ta*, GC and SB ranges corresponding to crop water stress classes.

Dates	Crop Water Stress Classes	*Ts-Ta* (℃)	GC (%)	SB (%)
8 August 2007	Non stressed	<0–0	40–63	27–51
	Moderately stressed	3–11	42–72	27–51
	Stressed	>11	28–51	35–62
28 August 2007	Non stressed	<0–6	63–91	65–80
	Moderately stressed	1–6	28–58	41–67
	Stressed	>10	23–47	57–78
30 July 2008	Non-stressed	none	none	none
	Moderately stressed	9–19	44–56	14–32
	Stressed	19–31	2–51	34–47

Well-watered conditions did not exist in 2008, due to the low rainfall and high mid-season temperatures (see Table 1), resulting in a higher crop ETc (Figure 1) than the irrigation system could meet. The resulting crop water stress classes assigned according to the HSI analysis corresponded to the resulting lint yield [29]. In 2007, yields in the HighIrr, LowIrr and dryland treatments were significantly different and were higher than the corresponding yields in 2008 (Figure 8, [29,30]). Yields in the irrigated treatments in 2008, which were classified as stressed or moderately stressed, were similar to the LowIrr treatment in 2007, which was classified as moderately stressed. The yield data supported the crop water stress classes assigned for each image acquisition year.

Figure 9 shows *Ts-Ta*, GC and SB plotted as three orthogonal coordinates, with *Ts-Ta* representing the surface energy balance, GC representing crop growth and SB representing the apparent wetness of the soil surface. Combinations of GC and SB data for the imagery for this date (8 August 2007) lie in horizontal triangular-shaped distributions layered according to the magnitude of the resulting energy balance, as indicated by *Ts-Ta*. The GC tended to peak at intermediate values of *Ts-Ta*. Increasing apparent soil moistness (*i.e.*, decreasing SB) generally was associated with decreasing *Ts-Ta*.

The HSI approach is able to discriminate between the crop water stress classes as inferred from the irrigation treatments used in this study and the reported yields. The additional new dimension (*i.e.*, SB) to the remotely sensed VITT approach [6] enabled the fusion of surface information (*Ts-Ta*, GC and SB) for detecting crop water stress and segregating bare soil surface from the cotton canopy. Moreover, a subtle boundary between non-stressed crop and moderately stressed crop (*i.e.*, between

values of zero and one for *Ts-Ta*) was revealed. This capability resulted because *Ts-Ta* was assigned to the H component, which is known to facilitate detecting slight changes in that component [28]. The result of this study indicates that SB helped discriminate the difference between the moderately stressed and stressed cotton crop, along with an ability to segregate the non-cropped bare soils from the cropped areas.

Figure 8. Lint yield for the three irrigation treatments in each year [29]. The standard error of estimates was calculated using the Procmixed model in SAS [30] with the irrigation treatment as the fixed effect and the year as a random effect. The yield difference between treatments greater than the least significant difference ($LSD_{0.05}$) is significant.

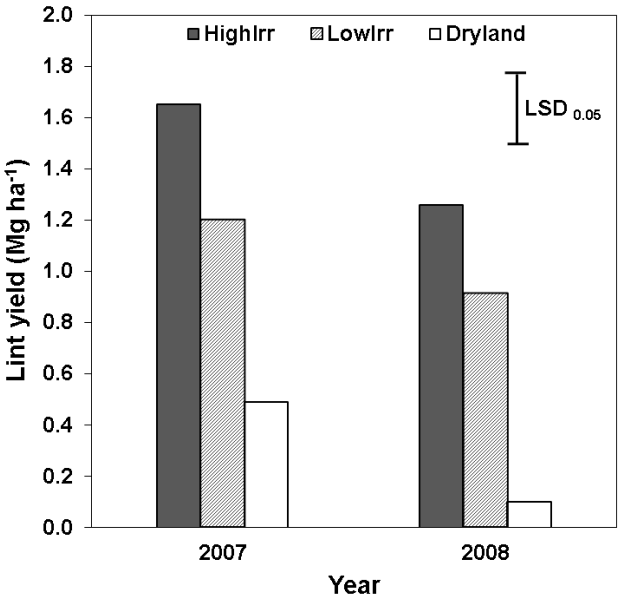

Figure 9. GC, SB and *Ts-Ta* plotted on three orthogonal axes. GC is associated with crop growth, SB with apparent soil moistness and *Ts-Ta* with the surface energy balance. Plotted data are for the 8 August 2007, image acquisition date.

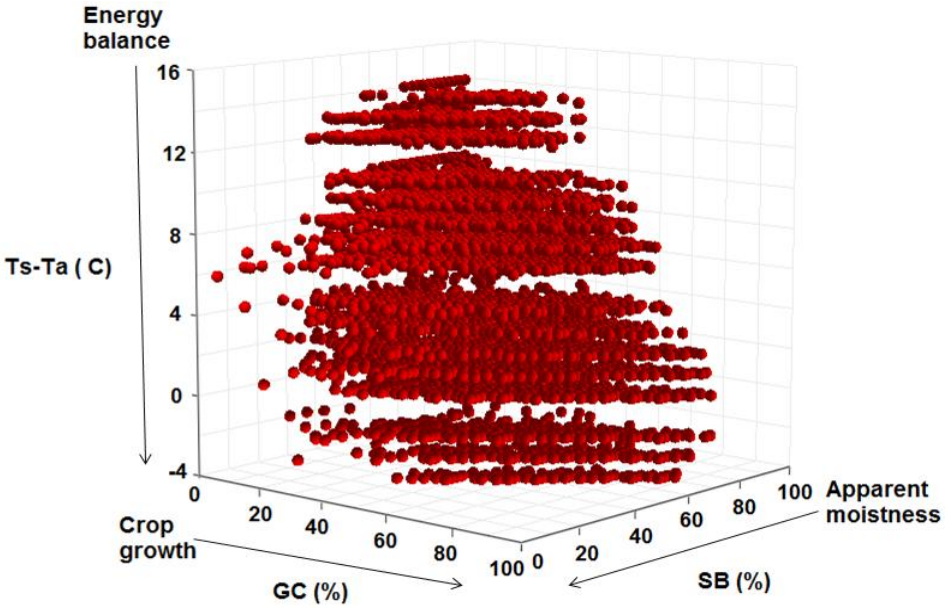

3.5. Crop Water Stress Analysis Using the VITT-Trapezoid Approach

Figure 10 shows a VITT-trapezoid analysis of crop water stress using GC and *Ts-Ta* data from Figure 5. The four corners of the trapezoid in terms of GC (Y-axis) and *Ts-Ta* (X-axis) were known using the bare soil surfaces from the SB analysis and their corresponding *Ts-Ta*. The absence of a pixel that represents a *Ts-Ta* value for 100% GC in this study was estimated by an energy balance method [31]. Notable in the VITT analysis is the observation that the non-vegetated bare soil surfaces are not distinctive in the crop stress classified image. The pink colors in Figure 10 represent stressed plants (moderately- to severely-stressed plants) with a completely dry soil background that corresponds to the moderately- to severely-stressed plants in 3D-CWSI (blue and pink representations in Figure 5). The VITT approach seems to classify the water stress levels, as indicated by ground truth and irrigation treatments, but detecting levels of stress spatially is not effective. For example, the northern part of the field that was 100% severely stressed in 2008 (shown in Figure 7C) is classified as both stressed and non-stressed crop with dry soil background in the VITT approach (Figure 10). Similar limitations were also reported in the literature for semi-arid applications [32].

Figure 10. Crop water stress classes for 2007 (**A**,**B**) and 2008 (**C**) using the Vegetation Index-Temperature Trapezoid (VITT) approach [6] and classes of stress according to the pixel location [31] within the trapezoid.

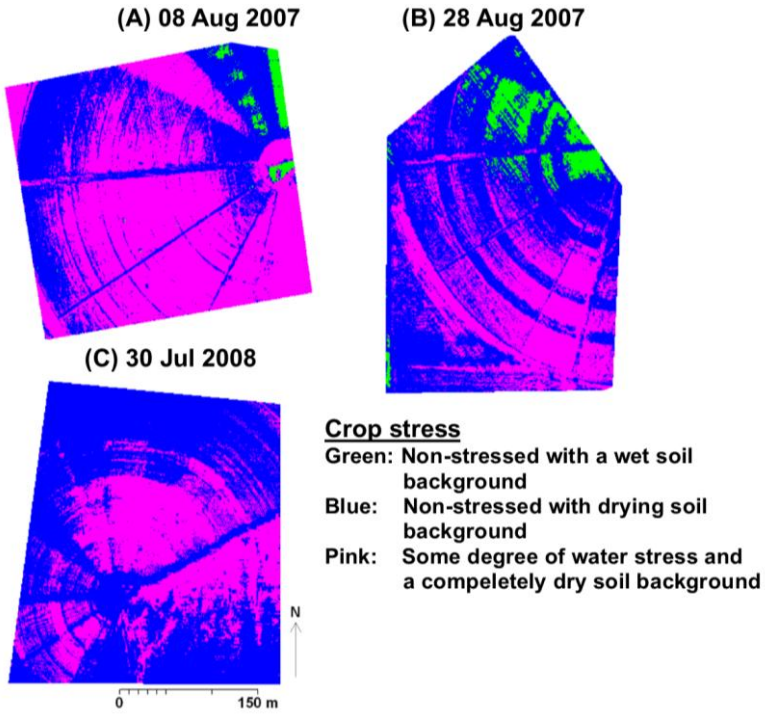

4. Conclusions

The HSI color composition method was able to assess the crop water stress of cotton crop from remote sensing observations of canopy cover (estimated using the PVI method), the energy balance characteristics of a surface (estimated by the difference between surface and air temperature) and the apparent moistness of the soil surface (indicated by a measure of SB). This assessment of crop water

stress in cotton was based on the applied irrigation treatments and resulting yields. This new approach utilizes readily available data (remotely sensed reflectance and temperature and measurements of air temperature) and provides an alternative way to determine crop water stress, even in situations of partial canopy cover without additional energy balance determinations (involving aerodynamic and canopy resistances).

SB as an additional dimension to GC and *Ts-Ta* (*i.e.*, the VITT trapezoid approach) shows promise in assessing the relative degree of water stress. This inclusion leads to a three-dimensional approach, by the HSI method. This approach evaluates water stress that is spatially consistent over years, as indicated by the water regime and ETc demand. Additional investigations may validate the approach to actual measurements of stress (as from ET measurements) and may reveal the accuracy and applicability of this approach.

Acknowledgments

The authors wish to acknowledge the USDA-ARS Ogallala Aquifer Initiative for supporting this project. We also thank South Plains Precision Ag Inc., of Plainview, TX, for the use of the aircraft that allowed the image acquisition with the TTAMRRS.

Author Contributions

Jessica Torrion conducted this study and wrote this paper. Stephan Maas provided guidance for data gathering/analysis, and edits. Wenxuan Guo supported this research for successful deployment of TTAMRRS as well as edits to this paper. James Bordovsky and Andy Cranmer helped the conduct of this research on the ground from planting to harvest. They provided crop management and yield data, plus, inputs in the methods section.

Conflicts of Interest

The authors declare no conflict of interest.

References

1. Jackson, R.D.; Idso, S.B.; Reginato, R.J.; Pinter, P.J. Canopy temperature as a crop water stress indicator. *Water Resour. Res.* **1981**, *17*, 1133–1138.
2. Jackson, R.D.; Pinter, P.J.; Reginato, R.J.; Idso, S.B. Detection and evaluation of plant stresses for crop management decisions. *IEEE Trans. Geosci. Remote Sens.* **1986**, *GE-24*, 99–106.
3. Wanjura, D.F.; Kelly, C.A.; Wendt, C.W.; Hatfield, J.L. Canopy temperature and water stress cotton crops with complete and partial ground cover. *Irrigation Sci.* **1984**, *5*, 37–46.
4. Pinter, P.J.; Hatfield, J.L.; Schepers, J.S.; Barnes, E.M.; Moran, M.S.; Daughtry, C.S.T.; Upchurch, D.R. Remote sensing for crop management. *Photogramm. Eng. Remote Sens.* **2003**, *69*, 647–664.
5. Ham, J.M.; Heilman, J.L.; Lascano, R.J. Soil and canopy energy balances of a row crop at partial cover. *Agron. J.* **1991**, *83*, 744–753.

6. Moran, M.S.; Clarke, T.R.; Inoue, Y.; Vidal, A. Estimating crop water deficit using relation between surface-air temperature and spectral vegetation index. *Remote Sens. Environ.* **1994**, *49*, 246–263.
7. Maas, S.; Rajan, N. Estimating ground cover of field crops using medium resolution multispectral satellite imagery. *Agron. J.* **2008**, *100*, 320–327.
8. Galvão, L.S.; Vitorello, I. Variability of laboratory measured soil lines of soils from southeasthern Brazil. *Remote Sens. Environ.* **1997**, *63*, 166–181.
9. Gerrard, J. *Fundamentals of Soils*; Taylor and Francis: London, UK, 2000; p. 230.
10. Idso, S.B.; Jackson, R.D.; Reginato, R.J.; Kimball, B.A.; Nakayama, F.S. The dependence of bare soil albedo on soil water content. *J. Appl. Meteorol.* **1975**, *14*, 109–113.
11. Skidmore, E.L.; Dickerson, J.D.; Schimmelpfennig, H. Evaluating surface-soil water content by measuring reflectance. *Soil Sci. Soc. Am. J.* **1975**, *39*, 238–242.
12. Twomey, S.A.; Bohren, C.F.; Mergenthaler, J.L. Reflectance and albedo differences between wet and dry surfaces. *Appl. Opt.* **1986**, *25*, 431–437.
13. Whiting, M.L.; Li, L.; Ustin, S.L. Predicting water content using Gaussian model on soil spectra. *Remote Sens. Environ.* **2004**, *89*, 535–552.
14. Maas, S.J.; Rajan, N. Normalizing and converting image DC data using scatter plot matching. *Remote Sens.* **2010**, *2*, 1644–1661.
15. Soil Survey Staff. *Custom Soil Resource Report 2008*. Available online: http://websoilsurvey.nrcs.usda.gov/app/WebSoilSurvey.aspx (accessed on 1 May 2008).
16. Porter, D.O.; Marek, T.; Howell, T.A.; New, L. *Texas High Plains Evapotraspiration Network TX A&M*; Univ. Sys. Agric. Res. and Ext. Centers: Bushland, TX, USA, 2006.
17. Nayak, S. Thermal Imagery And Spectral Reflectance Based System To Monitor Crop Condition. Master's Thesis, Texas Tech Univisity, Lubbock, TX, USA, 2005.
18. Huang, Y.; Thomson, S.J. Airborne multispectral and thermal remote sensing for detecting the onset of crop stress caused by multiple factors. *Proc. SPIE* **2010**, *7824*, doi:10.1117/12.864190.
19. Research Systems Inc. *The Environment for Visualizing Images*; *ENVI*, Research Systems, Inc.: Boulder, CO, USA. 2003.
20. Pohl, C.; Van Genderen, J.L. Multisensor image fusion in remote sensing: Concepts, methods and applications. *Int. J. Remote Sens.* **1998**, *19*, 823–854.
21. Jackson, R.D.; Pinter, P.J.; Reginato, R.J.; Idso, S.B. Hand-Held Radiometry. In *Agricultural Reviews and Manuals*; USDA: Oakland, CA, USA, 1980; pp. 1–66.
22. Richardson, A.J.; Wiegand, C.L. Distinguishing vegetation from soil background information. *Photogram. Eng. Remote Sens.* **1977**, *43*, 1541–1552.
23. Maas, S. Estimating cotton canopy ground cover from remotely sensed scene reflectance. *Agron. J.* **1998**, *90*, 384–388.
24. Koolhooven, W.; Hendrikse, J.; Nieuwenhauis, W.; Retsios, B.; Schouwenburg, M.; Wang, L.; Budde, P.; Nijmeijer, R. *Integrated Land Water Information System, ILWIS 3.31*; ITC: Eschede, The Netherlands, 2007.

25. McMaster, G.S.; White, J.W.; Weiss, A.; Baenziger, S.P.; Wilhelm, W.W.; Porter, J.R.; Jamieson, P.D. Simulating Crop Phenological Responses to Water Deficit. In *Response of Crops to Limited Water*; Ahuja, L.R., Reddy, V.R., Saseendran, S.A., Yu, Q., Eds.; CSSA, ASA, SSSA: Madison, WI, USA, 2008; pp. 277–300.
26. Ham, J.M.; Heilman, J.L. Aerodynamic and surface resistances affecting energy transport in a sparse crop. *Agric. For. Meteorol.* **1991**, *53*, 267–284.
27. Matthias, A.D.; Kustas, W.P.; Gay, L.W.; Cooper, D.I.; Alves, L.M.; Pinter, P.J., Jr. Aerodynamic parameters for a sparsely roughened surface composed of small cotton plants and ridged soil. *Remote Sens. Environ.* **1990**, *32*, 143-153.
28. Carper, W.J.; Lillesand, T.M.; Kiefer, R.W. The use of intensity-hue-saturation transformations for merging spot panchromatic and multispectral image data. *Photogramm. Eng. Remote Sens.* **1990**, *56*, 459–467.
29. Bordovsky, J.P.; Mustian, J.T.; Cranmer, A.M.; Emerson, C.L. Cotton-grain sorghum rotation under extreme irrigation conditions. *Appl. Eng. Agric.* **2011**, *27*, 359–371.
30. Little, R.C.; Milliken, G.A.; Stroup, W.W.; Wolfinger, W.W. *SAS for Mixed Models*; SAS Institute, Inc: Cary, NC, USA, 2006.
31. Clarke, T.R. An empirical approach for detecting crop water stress using multispectral airborne sensors. *HortTechnology* **1997**, *7*, 9–16
32. Wang, W.; Huang, D.; Wang, X.D.; Liu, Y.R.; Zhou, F. Estimation of soil moisture using trapezoidal relationship between remotely sensed land surface temperature and vegetation index. *Hydrol. Earth Syst. Sci.* **2011**, *15*, 1699–1712.